2013 IEEE/ASME International Conference on
Advanced Intelligent Mechatronics (AIM)
Wollongong, Australia, July 9-12, 2013

Design and Development of a Compact Hovercraft Vehicle

Soe Myat Hein[1] and Hwee Choo Liaw[2]

Abstract— **This paper presents the design and development of a compact one-seater hovercraft vehicle. In particular, the hovering and propulsion mechanisms are investigated. A mathematical model is derived to describe the dynamics of the proposed prototypes. Consequently, experimental studies are conducted to evaluate the proposed mechanisms. This development draws inspiration from meeting user requirements and aims to improve upon the currently available conventional designs of hovercrafts, also known as air cushion vehicles, for greater user-friendliness. From a wider perspective, over the course of history of study on hovercrafts, attention has converged mostly on large-scale vehicles in commercial and military sectors. Apart from hobbyists', little attention has been given to the development of compact light-weight hovercrafts, into which this paper will provide some valuable insights.**

I. INTRODUCTION

The study of hovercrafts, formerly known as "air cushion vehicles" (ACV), was led by a model in 1959, namely SR.N1, a hovercraft which hovered on a thin layer of air cushion underneath [1], [2]. This layer allowed the vehicle to stay clear of the underlying surface, thereby extending the realm of navigation to places and terrains which were previously not accessible by other conventional land and sea vehicles such as cars and ships. Since then, improvements to the existing designs which use air cushions were progressively made in such forms as Sidewall hovercrafts [3].

The majority of literature studies, in an attempt to provide smoother manoeuvrability and better stability, is, however, focused on the development of large-scale transport vehicles [2], [3]. As such, hovercrafts are better known for commercial and military purposes and the development for civilian objective has lagged behind; development of small-scale vehicles in this context has been restricted to concept-testing projects by academics and attempts by hobbyists [1]. The goal of the design process presented in the paper is thus to design and develop a compact one-seater hovercraft vehicle of small size, yet high performance, in accordance with insights drawn from our ethnographical research. Our study was conducted, as part of the design cycle, on the target user group consisting of daily commuters in urban locations. It was discovered that there is considerable demand for vehicles with added navigation capabilities, along the lines of hovercrafts. Moreover, users had requirements towards more compact size and high performance. These constraints are thus the primary guiding factors in the design and development of the hovercraft vehicle.

The pioneering models of hovercrafts made use of a plenum chamber, a pressurized region underneath the vehicle, to achieve a hovering effect [3]. However, the performance is limited in that the hovering height is minimal and thus, even low obstacles undermine movement. Later improvements using the concept of peripheral jet provided higher efficiency and lifting power [1]. Even with this improvement, low obstacles are difficult to overcome. The breakthrough to these problems arrived with the experimentation of a flexible skirt underneath the vehicle, which has been demonstrated to be able to reach a hovering height of $3.6\,ft$ on land and $4\,ft$ in sea. Later improvements focused on modifications of the skirt and resulted in better obstacle clearance and include such varieties as the convoluted skirt, bag skirt and segmented skirt, to name a few. However, these approaches are only effective on large-scale implementation and not suitable for compact sizes due to their bulkiness. In consideration of the afore-mentioned constraints, a design combining the concepts of peripheral jet, bag skirt and perforations is proposed for suitability in urban context. This design combines the stability found in large vehicles with compactness.

Propulsion in hovercrafts, on the other hand, has been traditionally implemented using marine propellers, air propellers or water jet as the single source of forward thrust or in combination of different methods [2]. Among them, air propellers are the dominant method in today's hovercraft designs. However, these propellers are large in size and pose a major constraint of design requirements. On the other hand, with technical advancements in power electronics, small-sized ducted fans driven by high-speed brushless motors are proposed for the required propulsive power.

The paper is organized as follows. Major aspects of the vehicle, hovering and propulsion mechanisms, are presented in Section II and III, respectively. Section II is divided into modelling, methodology, implementation, simulation and experimentation, whereas Section III is divided into modelling, methodology and experimentation. Finally, the conclusion is presented in Section IV.

II. HOVERING MECHANISM

A. Model of Hovering Mechanism

For comparison purposes, two prototypes (Prototype 1 and Prototype 2) were developed based on two different designs. Nonetheless, both of the prototypes are based on the same principles of fluid dynamics. Therefore, a single

*This work is supported by the Engineering Design and Innovation Centre (EDIC) through its Design-Centric Programme (DCP) at the National University of Singapore.

[1]S.M. Hein is with the DCP and the Department of Mechanical Engineering, National University of Singapore u0906179@nus.edu.sg, soetommy@gmail.com

[2]H.C. Liaw is with the EDIC, Faculty of Engineering, National University of Singapore englhc@nus.edu.sg

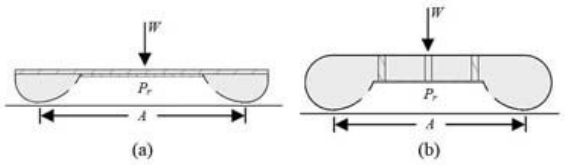

Fig. 1. Schematic drawing of (a) Prototype 1 (b) Prototype 2

representative mathematical model is used to describe them. Fig. 1 shows a schematic drawing of the prototypes, on which the mathematical model is derived, where W represents the total weight of the vehicle including the user on board, P_r is the gauge pressure of air medium inside the plenum chamber ultimately required for the vehicle to hover and A is the area of the plenum chamber bounded by the lowest points of the inflated skirt. Equations (1) to (4) provide a foremost analysis of the system:

$$W = (m_v + m_u)\, g \quad (1)$$

$$F = P_r\, A \quad (2)$$

$$F = W \quad (3)$$

$$P_r = \frac{(m_v + m_u)\, g}{A} \quad (4)$$

where m_v and m_u represent the masses of the vehicle and the user, respectively, g is the acceleration due to gravity, F is the upward lift provided by P_r. The operational state of the vehicle is when the system is in equilibrium (3), whereby the total imposed weight is balanced by the upward lift. The necessary lift is provided by required amount of pressure P_r which is derived through substitution of (1) and (2) into (3).

In order to achieve the required pressure P_r inside the plenum chamber, the working fluid has to undergo a series of minor losses. The trajectory that the air medium has to travel within the skirt, which traces from the inlet through the perforations of the skirt to the plenum chamber, is modelled as a pipeline, due to the similarity of the cross-sectional geometry of the trajectory of the air medium. Working fluid, as it travels along the trajectory, experiences head loss due to friction losses as well as minor losses due to 90° sharp bends [4]. In the model, minor losses at the bends are contributed by the flow separation due to the abrupt change in flow direction and the formation of secondary flow. They occur at three distinct locations: at each inlet, at each corner of the skirt, and finally at each perforation. Meanwhile, friction losses due to the surface roughness of the skirt material is incurred along the trajectory. Therefore, the additional pressure that must be supplied to account for these losses, P_d, is described by the following set of equations:

$$H_f = f\,\frac{L_a}{d}\,\frac{{V_a}^2}{2g} \quad (5)$$

$$H_p = 3\,K\,\frac{{V_a}^2}{2g} \quad (6)$$

$$H = H_f + H_p \quad (7)$$

$$P_d = \rho\, g\, H \quad (8)$$

$$P_d = \rho\,\frac{{V_a}^2}{2}\,(f\,\frac{L_a}{d} + 3\,K) \quad (9)$$

where H_f represents the head loss due to friction, H_p is the head loss due to minor losses at the bends, H is the total head loss incurred, f is the friction factor, L_a is the average distance travelled by the air medium, d is the diameter of the cross-section of the trajectory, V_a is the average velocity of the flow, g is the acceleration due to gravity, K is the nominal loss coefficient of the bend and ρ is the density of atmospheric air. Equations (5) and (6) are substituted into (7), and then into (8) to arrive at the total pressure drop incurred (9). Average velocity V_a is estimated to be the average of speed of air medium between the inlet and the outlet while average distance L_a is estimated as the distance from the inlet to the centre of the vehicle. The value of nominal loss coefficient K is a function of the angle and radius of curvature of the bend [5], and can rise up to 1.5 at 90° bends [6]. The value of K has a multiple of 3 based on the assumption that the working fluid has to pass three sharp bends.

The total gauge pressure that must be supplied P_t is the combination of the required pressure P_r and the inherent pressure drop P_d, as shown in (10) and (11).

$$P_t = P_r + P_d \quad (10)$$

$$P_t = \frac{(m_v + m_u)\, g}{A} + \rho\,\frac{{V_a}^2}{2}\,(f\,\frac{L_a}{d} + 3\,K) \quad (11)$$

$$P_t = \rho\,\frac{{V_i}^2}{2} \quad (12)$$

As can be seen in (12), the required input gauge pressure is supplied by increasing the velocity of working fluid at the inlet to the required velocity V_i.

$$H_t = \frac{P_t}{\rho\, g} \quad (13)$$

$$\dot{W}_t = \rho\, g\, Q\, H_t \quad (14)$$

$$\eta = \frac{\dot{W}_t}{\dot{W}_i} \quad (15)$$

$$\dot{W}_i = \frac{Q}{\eta}\left\{\frac{(m_v + m_u)\, g}{A} + \rho\,\frac{{V_a}^2}{2}(f\,\frac{L_a}{d} + 3\,K)\right\} \quad (16)$$

In the above set of equations, H_t is the increase in total head of the incoming working fluid, an equivalent of the total pressure supplied P_t, Q is the total volume flow rate into the system, through the inlets, $\dot{W}_t$ is the total power gained by the system, $\dot{W}_i$ is the input power consumed by the fans, and η is the efficiency of useful energy obtained by the system. Combining equations (13) through (15) results in (16) which describes the required power input $\dot{W}_i$ as a function of a range of variables including vehicle dimensions, properties of working fluid which is atmospheric air and the total weight. Equation (16) also takes into account the efficiencies and losses present in the system in both electrical and fluid dynamics context.

For the schematics shown in Fig. 1, the mathematical model (16) prescribes that the input power is proportional to the total weight imposed and the total volume flow rate

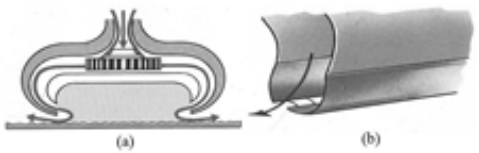

Fig. 2. (a) Peripheral jet (b) Bag skirt, [1]

into the inlets. This implies that fans designed to provide a higher volume flow rate for a given rpm should be selected as they can perform better at lesser power requirements. On the other hand, the equation dictates that the performance of the system is greatly affected by the head losses at the bends, as evidenced by the multiple of 3 to the nominal loss coefficient.

B. Methodology and Implementation of the Model

The proposed model (16) is designed and implemented by incorporating the concepts of peripheral jet, bag skirt and perforations for compactness. A study [1] has shown that the concept of peripheral jet, as shown in Fig. 2(a), circulates the air to the outer rim of the vehicle for increased efficiency compared to the conventional concept of channelling air directly into the plenum chamber under the vehicle. In addition to the concept of peripheral jet, a bag skirt, exemplified in Fig. 2(b), is affixed around the rim for air to accumulate first before eventually exiting into the plenum chamber through the perforations along the length of the bag skirt. Once inside the plenum chamber, air accumulates and builds up pressure to provide the required upward lift, enabling the vehicle to hover. Accumulation of air inside the skirt is designed to ensure a nearly-enclosed plenum chamber, the effectiveness of which increases for smaller size and greater downward force such as weight.

Two prototypes (Prototype 1 in Fig. 3 and Prototype 2 in Fig. 5) were developed sequentially to observe and compare the performances of the two different designs. In Prototype 1, air is directed into the skirt through two inlets and allowed to circulate around the rim inside the skirt, eventually making the exit as it encounters perforations along the path of travel. Once inside the plenum chamber, pressurized air provides the upward lift force required to hover. On the other hand, as pressure continues to build up due to continued supply of air, some of the air leaks out from the plenum chamber into the atmosphere from underneath the skirt, as can be seen in Fig. 4 and Fig. 6. The skirt remains inflated throughout operation due to continued supply of air through the two inlets with the help of two fans delivering a constant mass flow rate.

Thus, the hovering height by which the vehicle is lifted up is affected by the inflation of the skirt around the rim. While the vehicle is in the state of hovering, total contact surface area is reduced because parts of the vehicle are lifted up and no longer in contact with the surface, leading to less friction.

Prototype 1 successfully hovers under the payload of 50 kg, a presumed equivalent of a humans weight. However,

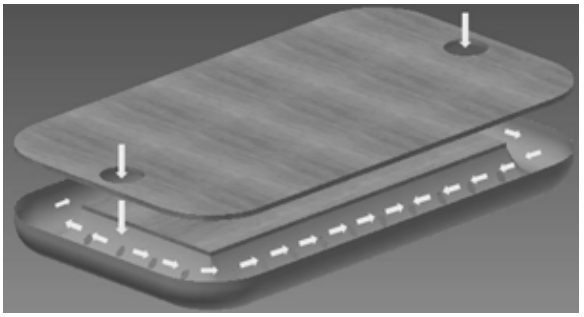

Fig. 3. Prototype 1 (exploded view, isometric view) showing indicative air flow in the skirt

Fig. 4. Prototype 1 (cross-sectional view)

the design used in Prototype 1 is ineffective in providing stability. Under the load of a human standing at the centre of the vehicle, the vehicle is able to hover as expected; however, the vehicle is vulnerable to small lateral displacements of the centre of gravity away from the centre of the vehicle, in which cases, there is strong tendency for the vehicle to topple to the side and touch the ground. Thus, Prototype 2 is introduced as an improvement to Prototype 1 and designed in such a way to provide the required reaction moment to stabilize the vehicle in response to lateral displacements.

Prototype 2, shown in Fig. 5, is based on the same principles of fluid dynamics as Prototype 1. The major change in design is the addition of the empty compartment inside the vehicle body in order to enable air to reach the rim of the vehicle not only by travelling along the rim but also by spreading out towards the rim through the empty compartment. The benefit of this modified concept is that when the vehicle is toppled to a side, it is now easier for air inside the compartment to rapidly reach the toppled side to inflate the skirt back to its operational condition. The addition of the empty compartment provided greatly improved stability whereby the user can comfortably and speedily adjust himself back to better configuration.

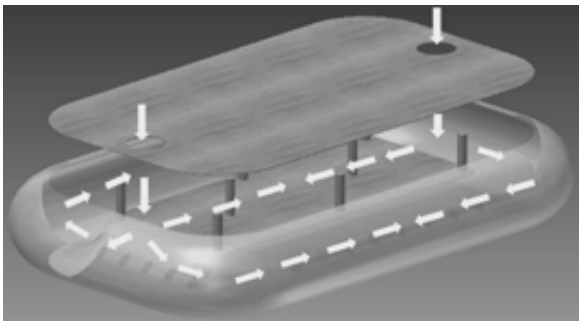

Fig. 5. Prototype 2 (exploded view, isometric view) showing indicative air flow in the skirt

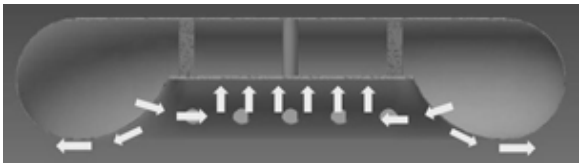

Fig. 6. Prototype 2 (cross-sectional view)

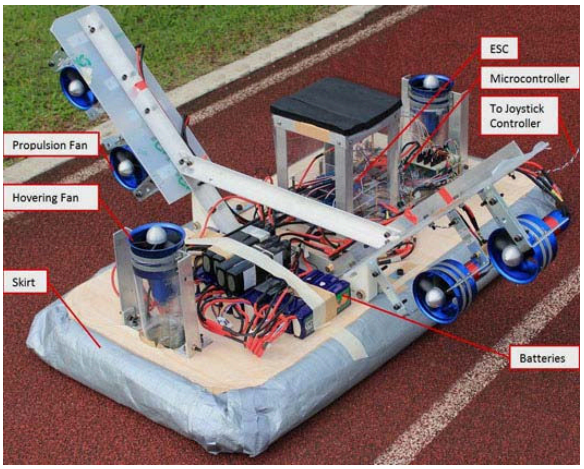

Fig. 7. Implementation of Prototype 2 showing components of the vehicle

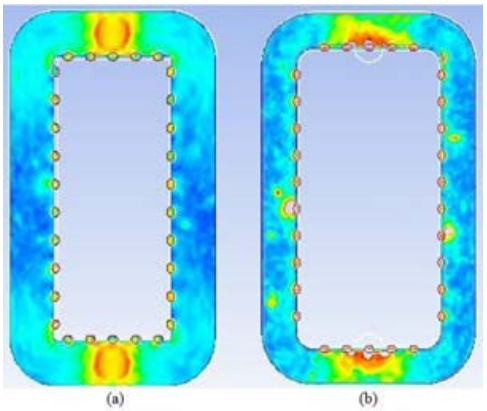

Fig. 8. CFD simulation results: (a) Prototype 1 (b) Prototype 2

TABLE II
HOVERING PERFORMANCE

		Prototype 1	Prototype 2
Maximum Payload		$70\,kg$	$55\,kg$
Hovering Height	Without Payload	$4.5\,cm$	$5.5\,cm$
	Payload $= 50\,kg$	$1.3\,cm$	$1.0\,cm$

The major components of Prototype 2, shown in Fig. 7, are hovering and propulsion fans, skirt, microcontroller, electronic speed controllers (ESC) and batteries. Table I tabulates the specifications of the prototypes. To realize the hovering capability of the vehicle, high-speed electric brushless DC motors are utilized for the required mass flow rate; they are powered by high-capacity, high-discharge Lithium Polymer batteries and controlled using a joystick controller.

C. Computational Fluid Dynamics (CFD) Simulations

Computational Fluid Dynamics simulations are executed to provide a visual aid in analysing the fluid dynamics inside the vehicles. Firstly, 3D models were created using AutoDesk Inventor [7] as shown in Fig. 3 to Fig. 6. Secondly, they are exported into Gambit [8], a mesh-generation software package, where the geometry is further modified and the corresponding mesh models are generated. The mesh is generated using the element Tet/Hybrid with type TGrid, which creates the mesh primarily with tetrahedral elements and other elements such as hexahedral or pyramidal elements where appropriate. This option provides an unstructured mesh with a mix of elements, suitable for complex geometries. During this pre-processing stage, boundary conditions such as air inlets, pressure outlets and wall boundaries are also defined. Thirdly, the pre-processed geometry is exported into Fluent Solver [9], a flow modelling and simulation software package distributed by ANSYS, to execute the flow simulations and analyse results in the post-processing stage.

Simulation results are shown in Fig. 8 and the colour contours represent the absolute velocity of air at the plane level with the outlets. Results predict significant head loss of incoming air due to a considerable reduction in velocity, and thus the dynamic pressure, as expected from the proposed model (16). Such loss is evidenced by the drastic change in colour contour at the inlets at either end and at the corners along the length of the skirt.

TABLE I
SPECIFICATIONS OF PROTOTYPES

	Prototype 1	Prototype 2
Dim. (Length $\times$ Width)	$1220\ mm \times 700\ mm$	
Mass of Vehicle	$10.5\,kg$	$17\,kg$
Rating of Hovering Motor	$22.2\,V$, $85\,A$, $1.5\,kW$, $42\,krpm$	
Rating of Propulsion Motor	$37\,V$, $92\,A$, $3.0\,kW$, $45\,krpm$	

D. Experimentation

Experimental results on Prototype 1 and Prototype 2 are presented in Table II and Fig. 9, showing the hovering performance of the vehicle under different payloads. The power input to the fans is set to 25% duty cycle. Under such circumstance, a gradual decrease in hovering height, the distance between the bottom of the vehicle and the ground, was observed on increasing payload.

III. PROPULSION MECHANISM

A. Model of Propulsion Mechanism

A second-order linear system is used to model the propulsion system. Fig. 10 shows the free-body diagram of the model and it can be described by (17) to (19),

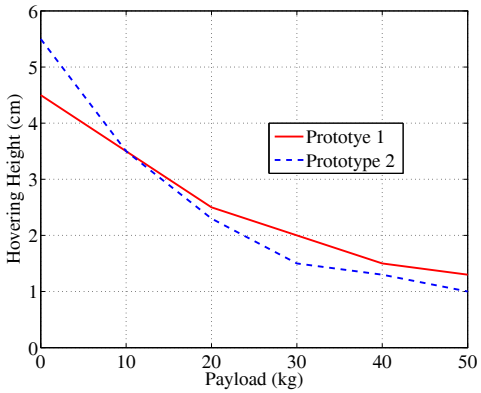

Fig. 9. Hovering height vs payload

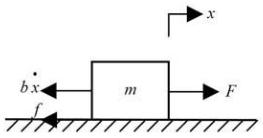

Fig. 10. Free-body diagram of the model of propulsion system

$$m\,\ddot{x} = F_e \tag{17}$$

$$F_e = F - b\,\dot{x} - f \tag{18}$$

$$m\,\ddot{x} + b\,\dot{x} = F - f \tag{19}$$

where x represents the linear displacement, $\ddot{x}$ is the acceleration of the system, m is the total mass of the system, b is the damping coefficient, F_e is the external force acting on the system, F is the total forward thrust supplied by the fans and f is the friction acting on the system. Equation (18) indicates the forward thrust by the fans is opposed by the forces due to damping and friction. Substitution of (18) into (17) results in (19), which describes the dynamics of the system. Friction in this model acts in two forms, namely static friction and dynamic friction during the static and dynamic states, respectively. It is understood that hovercrafts operate through reducing friction by means of a small layer of air underneath the skirt. During operation, the value of friction coefficient is greatly affected by the hovering height of the vehicle.

B. Propulsion Methodology

Historically, propulsion in hovercrafts is implemented in many forms and combinations. One of the earliest methods of propulsion was to tilt the vehicle by pitching the vehicle forward and nose-down. The forward thrust is derived through the resultant pressure force in the plenum chamber. Later developments include use of marine and air propellers, ducted fans and wheels. Among them, air propellers are the most common means of propulsion. In particular, hovercrafts developed primarily for overwater travels used marine propellers and those developed for overland purposes used wheels, respectively, in combination with air propellers. They are then again used together with vertical or inclined rudders for steering [10], [11].

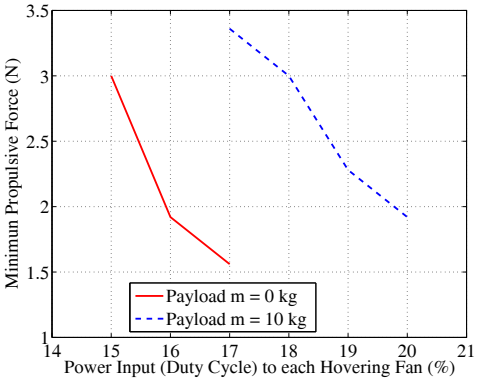

Fig. 11. Minimum propulsive force required to set into motion

A simplistic method of propulsion employing ducted fans actuated by extremely high-speed electric motors is proposed to implement the proposed model (19). Each of the propulsion fans selected operates at up to $45\,krpm$ at a mere size of $90\,mm$; thus, a high mass flow rate is achieved resulting in high thrust of up to $4.9\,kg$ force from each fan. A total of four fans were utilized during the development and experiments were conducted based on Prototype 2, as shown in Fig. 7. Specifically, the fans were affixed laterally with two on each side; thus, forward motion is theoretically achieved when equal thrust is provided by each fan and steering motion is achieved through differential thrust.

C. Experimentation

Experiments were conducted based on Prototype 2. The power requirement to the propulsion fans for motion was investigated. This was done by measuring the minimum propulsive forces required to overcome static friction for certain amounts of power input to the hovering fans. The experiment was repeated for two cases: with and without the payload of $10\,kg$. The fans were controlled by PWM driving signals operating between $1\,ms$ and $2\,ms$. Therefore, the power input to the hovering fans is described by the percentage form of the PWM duty cycle from $0\%\,(1\,ms)$ to $100\%\,(2\,ms)$. As shown in Fig. 11, it was observed that higher input power to the hovering fans provides a thicker layer of air underneath; this reduces the friction and thus the required forces to set into motion.

From the results, it is understood that by increasing the payload, the static friction will rise and a higher propulsive force is needed to move the vehicle. Furthermore, it was observed that for a given payload, if the power input to the hovering fans is increased beyond a certain duty cycle, the friction will be significantly reduced. At this point, a very small amount of propulsive force is required to overcome friction. On the other hand, if power input is less than a certain value, the static friction will reach a very high amount. In such case, the propulsive force needed will be extremely high to overcome the static friction.

$$\mu_s = \frac{F}{m\,g} \tag{20}$$

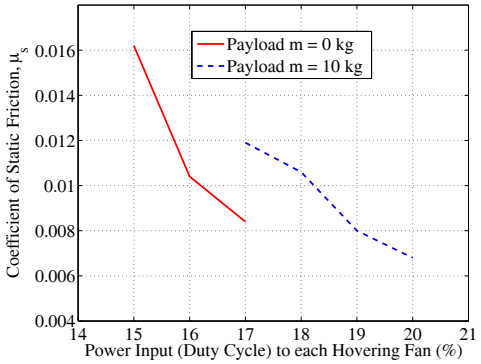

Fig. 12. Effective coefficient of static friction vs power input

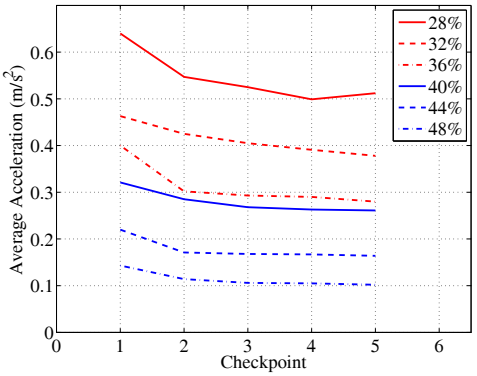

Fig. 14. Average acceleration of vehicle

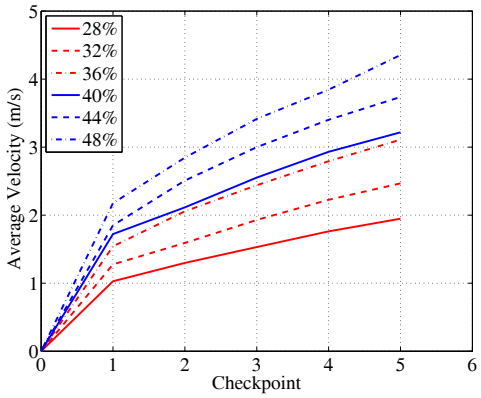

Fig. 13. Average velocity of vehicle

In equation (20), μ_s represents the coefficient of static friction and m is the total mass of the vehicle. Without payload, the value of μ_s is found to range from 0.0084 to 0.0162 whereas with the payload of $10\,kg$, it ranges from 0.0068 to 0.0119 with decreasing power to hovering fans, as shown in Fig. 12.

The performance of the vehicle has been evaluated through further experiments which map the average velocity and average acceleration of the vehicle with respect to different levels of power supplied to the propulsion fans expressed in percentage of duty cycle, as shown in Fig. 13 and Fig. 14. The averages are calculated over the total cumulative distance travelled which is measured by the number of checkpoints passed; each checkpoint is 3.7m long.

Fig. 11 to Fig. 14 describes the fundamental relationships that are central to the performance of the vehicle. The performance in overall is primarily affected by the interplay of power input to the two systems: hovering and propulsion systems. Naturally, the sequential stage of development is the implementation of the steering system and formulation of controls for smooth steering and navigation such as course-keeping of the underactuated hovercraft by eliminating sway velocity [12] and maintaining correct orientation of the vehicle at the lack of friction [13].

IV. CONCLUSIONS

A novel form of a compact one-seater hovercraft has been proposed, analysed and implemented. In this study, a mathematical model, in the context of the hovering and propulsion capabilities, has been derived and investigated. The proposed hovercraft serves as an improvement over the conventional forms, from which an electric-operated hovercraft can be realized.

Experimental results have verified feasibility in terms of actual implementation. It is also found that the proposed design offers the functionalities of a vehicle, despite at a much smaller scale. With the realization of the hovering and propulsion systems, the paper contributes yet another exciting new entry to the rich variety of existing transportation systems.

REFERENCES

[1] B. Gunston, Ed., *Hydrofoils and Hovercraft New Vehicles for Sea and Land*. London: Albus Book, 1969, pp 89–109.

[2] J. R. Amyot, Ed., *Hovercraft Technology Economics and Applications*. Amsterdam, The Netherlands: Elsevier Science Publishers, 1989.

[3] L. Yun and A. Bliault, Eds., *Theory and Design of Air Cushion Craft*. London: Arnold, 2000, pp 169–179.

[4] Y. A. Cengel and J. M. Cimbala, Eds., *Fluid Mechanics Fundamentals and Applications*. New York, NY: McGraw-Hill, 2010.

[5] P. Koch, "Comparisons and choice of pressure loss coefficients, z for ductwork components," *Building Services Engineering Research and Technology*, vol. 22, no. 3, pp. 167–183, June 2001.

[6] F. M. White, Ed., *Fluid Mechanics*. New York, NY: McGraw-Hill, 2011.

[7] 3D CAD and simulation for mechanical design. [Online]. Available: http://usa.autodesk.com/autodesk-inventor/,[Jan.17,2013].

[8] GAMBIT documentation suite. [Online]. Available: http://cdlab2.fluid.tuwien.ac.at/LEHRE/TURB/Fluent.Inc/gambit2.1/help/index.html,[Jan17,2013].

[9] ANSYS Fluent. [Online]. Available: http://www.ansys.com/Products/Simulation+Technology/Fluid+Dynamics/Fluid+Dynamics+Products/ANSYS+Fluent,[Jan17,2013].

[10] L. Chia and S. Omori, "Direction and lift control for hovercraft," U.S. Patent 5 096 012, March 17, 1992.

[11] H. Stiegler, "Steering gear for a hovercraft," U.S. Patent 5 520 260, May 28, 1996.

[12] J. Zhao and J. Pang, "Trajectory control of underactuated hovercraft," in *8th World Congress on Intelligent Control and Automation (WCICA)*, 7–9 July 2010, pp. 3904–3907.

[13] C. Wang, "Orientation control of hovercraft systems via an smflc and image-guided techniques," in *IEEE International Conference on Fuzzy Systems (FUZZ)*, 27–30 June 2011, pp. 1138–1142.